ChemComm

Accepted Manuscript

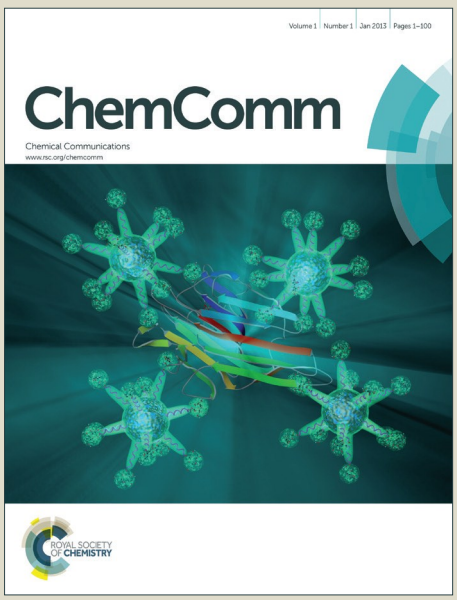

ROYAL SOCIETY OF CHEMISTRY

www.rsc.org/chemcomm

Journal Name

COMMUNICATION

An internal charge transfer-DNA platform for fluorescence sensing of divalent metal ions

Received 00th January 20xx,
Accepted 00th January 20xx

DOI: 10.1039/x0xx00000x

www.rsc.org/

Darian J.M. Blanchard and Richard A. Manderville*

Replacement of guanine (G) nucleobases within G-quadruplex (GQ) folding oligonucleotides with push-pull fluorescent 8-arylvinyl-dG residues provides diagnostic emission signalling for divalent metal ion binding.

The design of specific and sensitive fluorescent metal ion sensors is an ongoing challenge with significant opportunities. Metal ion sensors are needed to perform real-time, *in situ* studies of cellular metal ions and to provide on-site toxic metal detection platforms for environmental contamination. The fluorescent sensor should be selective for a specific metal ion and a turn-on emission response or shift in excitation/emission wavelengths is preferred over a turn-off emission-quenching response.[1] For biological systems, the fluorescent probe must also be water-soluble and nontoxic.[1]

Both synthetic small molecules and biomolecule-based fluorescent constructs have been developed for detecting metals of interest.[2] The internal charge transfer (ICT) mechanism has been widely exploited for metal ion sensing by fluorescent small molecules.[2-5] In this design the metal ion chelating fluorophore is a strong "push-pull" π-electron system that undergoes ICT to afford a long emission wavelength. However, when the fluorophore binds to the metal ion, the donor ability is diminished and a hypsochromic (blue) shift in the emission spectra is observed.[2-5] DNA is widely used in biomolecule-based constructs because it is naturally water-soluble, biocompatible and relatively easy to synthesize with modifications being readily introduced during the synthesis. Popular DNA detection platforms include metal-assisted DNAzyme catalysis,[6-8] or metal/nucleobase interactions.[9-11] DNAzymes can achieve extremely high metal ion sensitivity, but require *in vitro* selection to generate, which can be a labor intensive erroneous task. Many metal/nucleobase platforms are constructed with guanine (G)-rich DNA, which in the presence of certain metal ions can fold into G-quadruplex (GQ) structures. GQ-based fluorescent metal ion sensors typically employ an external dye that emits when bound to the GQ structure,[12-15] or end-labeled oligonucleotides[16,17] that provide an emissive response when the probes are brought into close contact upon intramolecular GQ folding. These platforms are potentially prone to false positives, as the fluorescent signal responds to the change in DNA topology and is insensitive to the nature of the metal ion present in the central cavity of the G-tetrad structure.

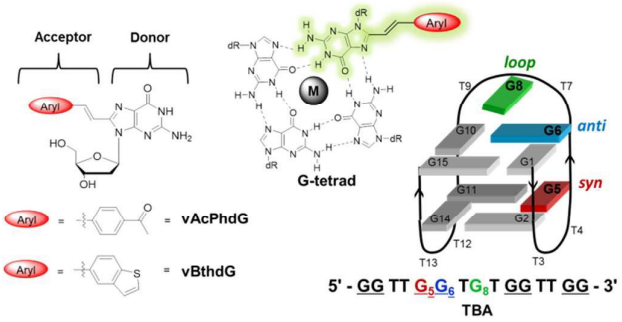

Fig. 1 Structures of donor-acceptor probes, G-tetrad and TBA.

In this study, we present the utility of two ICT nucleobase probes 8-(4"-acetylstyryl)-2'-deoxyguanosine (vAcPhdG) and 8-vinyl-benzo[*b*]thienyl-dG (vBthdG, Fig 1) for monitoring divalent metal ion binding within the antiparallel GQ produced by the 15-mer thrombin binding aptamer (TBA, Fig. 1).[18] The probes differ in the nature of their ICT states.[19] The vAcPhdG probe exhibits quenched emission at 585 nm in water (Φ_{fl} = 0.03) that is ascribed to a twisted ICT state, while the vBthdG probe favors a planar delocalized ICT state with relatively bright emission in water at 473 nm (Φ_{fl} = 0.29).[19] Based on the ICT mechanism for metal ion detection,[2-5] it was anticipated that the emission of vAcphdG and vBthdG would change in response to metal ion binding by the donor dG component within the central cavity of the G-tetrad upon GQ folding by TBA (Fig. 1). Furthermore, TBA can produce a stable

Departments of Chemistry & Toxicology, University of Guelph, Guelph, Ontario, Canada N1G 2w1. E-mail: rmanderv@uoguelph.ca
Electronic Supplementary Information (ESI) available: Fig S1A, S1B discribed in the text. See DOI: 10.1039/x0xx00000x

antiparallel GQ in the presence of potassium (K^+)[18,20] and the divalent metal ions barium (Ba^{2+}),[21] strontium (Sr^{2+})[21-23] and lead (Pb^{2+}).[24-27] This provided an opportunity to measure the emissive response of the push-pull probes at various TBA positions (G_5 (*syn*), G_6 (*anti*) or G_8 (loop), Fig. 1) as a function of metal cation within the two G-tetrads. Here we describe the first application of an ICT-GQ based aptasensor for the detection of divalent metal ions.

Solid-phase DNA synthesis was used to generate modified TBA (mTBA) containing vAcPhdG or vBthdG at the various positions (full synthetic details of vAcPhdG and vBthdG, their phosphoramidites and MS spectra of mTBA have been previously published[19,28]). The mTBA samples were studied using UV-thermal denaturation, circular dichroism (CD) and fluorescence spectroscopy.[29] Thermal melting parameters of the mTBA GQ structures are presented in Table 1. Native TBA (dG in Table 1) produces a more stable antiparallel GQ with the divalent metal ions tested[21,24] than in the presence of K^+ with the order in T_m being Sr^{2+} > Pb^{2+} > Ba^{2+} > K^+ under our experimental conditions. For the mTBA samples, a similar trend in T_m values was observed. The vAcPhdG probe had a stabilizing influence on GQ stability when inserted into *anti*-G_6 (ΔT_m 2.5 – 5.5 °C), while vBthdG was strongly destabilizing at the same position (e.g. ΔT_m = −15.5°C). Both probes had little impact on GQ stability at *syn*-G_5 and a destabilizing influence when inserted into the loop-G_8 position.

TBA produces an antiparallel GQ structure in K^+-solution with negative and positive bands at ~ 265 and 293 nm, respectively.[20] The divalent metal ions tested are known to cause the positive band at ~ 293 nm to shift to longer wavelengths, ~ 300 nm for Sr^{2+} and Ba^{2+},[21] and 312 nm for Pb^{2+}.[24] Displayed in Figs. 2A and 2B are representative CD curves for the vAcPhdG_5- and vBthdG_5-mTBA GQs with the various metal ions. Characteristic CD spectra for the antiparallel GQ structure were observed, confirming that the probes did not disrupt GQ folding. The positive band at 293 nm for the GQ with K^+ ion exhibited the expected shifts to longer wavelength with the divalent metal ions. CD spectra for the other mTBA samples were essentially identical (spectra not shown).

Table 1 UV thermal melting parameters[a]

mTBA	T_m (ΔT_m)[b]			
Probe	K^+	Ba^{2+}	Sr^{2+}	Pb^{2+}
dG	53.5	56.5	60.0	58.0
vAcPhdG_5	51.0 (−2.5)	56.5 (0.0)	58.0 (−2.0)	56.5 (−1.5)
vAcPhdG_6	56.0 (2.5)	62.0 (5.5)	64.5 (4.5)	61.0 (3.0)
vAcPhdG_8	50.5 (−3.0)	52.5 (−4.0)	54.5 (−5.5)	52.0 (−6.0)
vBtdG_5	51.5 (−2.0)	59.0 (2.5)	60.0 (0.0)	61.0 (3.0)
vBtdG_6	42.5 (−11.0)	42.0 (−14.5)	47.0 (−13.0)	42.5 (−15.5)
vBtdG_8	50.5 (−3.0)	54.5 (−2.0)	59.0 (−1.0)	53.5 (−4.5)

[a] T_m values of GQ structures (6 μM) were recorded with heating ramps of 0.5 °C/min (5 ramps) at 295 nm for K^+, Ba^{2+} and Sr^{2+} and 303 nm for Pb^{2+}; all T_m values in °C were reproducible within 3%. [b] ΔT_m = T_m (mTBA) – T_m (native TBA).

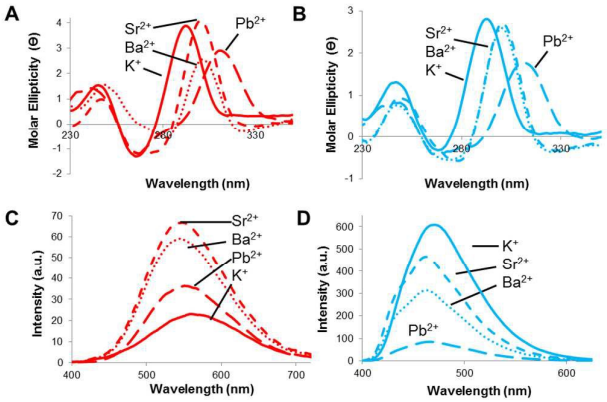

Fig. 2 CD spectral overlays (A,B) and metal-dependent emission spectra (C,D) of vAcPhdG_5-(red traces) and vBthdG_5-mTBA (blue traces) GQs in the presence of K^+ (solid traces), Ba^{2+} (dotted traces), Pb^{2+} (long-dashed traces) and Sr^{2+} (short-dashed traces) at 10 °C in aqueous buffer. (A),(C) vAcPhdG_5-mTBA GQs (B),(D) vBthdG_5-mTBA GQs.

The metal-dependent emissive response of vAcPhdG_5-mTBA upon GQ folding (Fig. 2C) demonstrated hyperchromic (increased intensity) and hypsochromic (blue) shifts in response to divalent metal ion binding in the order Sr^{2+} > Ba^{2+} > Pb^{2+} compared to the K^+-GQ (solid red trace). For the Sr^{2+}-GQ a 3-fold increase in emission intensity (I_{rel} value) coupled with a 15 nm blue-shift in emission wavelength ($\Delta\lambda_{em}$ value) compared to the K^+-GQ was observed. Values for I_{rel} and $\Delta\lambda_{em}$ for the other mTBA samples are provided in Fig. S1A (ESI). At each position, the Sr^{2+}-GQ provided the greatest I_{rel} response with Pb^{2+} providing the weakest; the GQ containing Ba^{2+} displayed similar or greater $\Delta\lambda_{em}$ values to that of Sr^{2+}. Of the mTBAs tested, the greatest probe response occurred at *syn*-G_5.

In contrast to the turn-on emissive response to divalent metal ion binding displayed by the vAcPhdG probe, the vBthdG_5-mTBA sample exhibited quenched emission (Fig. 2D) in the order Pb^{2+} > Ba^{2+} > Sr^{2+} compared to the K^+-GQ (solid blue trace). For the Pb^{2+}-GQ a 7.5-fold decrease in emission intensity compared to the K^+-GQ was observed. Divalent metal ion binding by vBthdG_5-mTBA also caused a blue-shift in emission wavelength with the greatest response occurring at *syn*-G_5 (Fig. S1B, ESI), as noted for the positional-dependent response of the vAcPhdG probe. Thus, the two ICT probes display different emission sensitivities to divalent metal ion binding. The turn-on emission response exhibited by the vAcPhdG_5 probe can distinguish Sr^{2+} or Ba^{2+} from K^+ (Fig. 2C), while the turn-off response by vBthdG_5 clearly distinguishes Pb^{2+} from K^+ (Fig. 2D). This emission sensitivity permitted the utility of fluorescence titration experiments (Fig. 3) to determine dissociation constants (K_d) for divalent metal ion binding by the mTBA samples.[30]

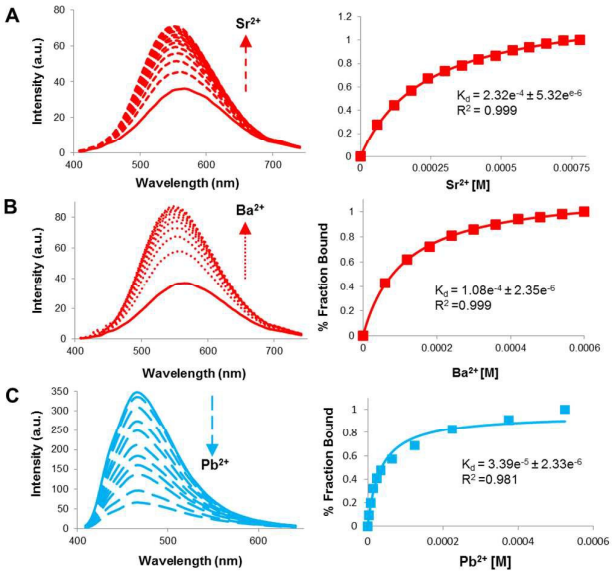

Fig 3 Divalent metal ion emission titrations carried out with 6 μM mTBA at 25°C. (A) vAcPhdG$_5$-mTBA with $SrCl_2$ in 50 mM Na^+-phosphate, pH 7, 100 mM NaCl, (B) vAcPhdG$_5$-mTBA with $Ba(OAc)_2$ in 50 mM Na^+-phosphate, pH 7, 100 mM NaCl, (C) vBthdG$_5$-mTBA with $Pb(NO_3)_2$ in 10 mM Tris/acetate pH 6.4. Initial emission spectrum of mTBA depicted by solid line; dashed/dotted lines depict emission traces upon successive addition of metal in 5 min intervals.

The emission titration data afforded K_d values of 232 μM for Sr^{2+}, 108 μM for Ba^{2+} and 34 μM for Pb^{2+} under our experimental conditions. For comparison, the K_d of TBA and Sr^{2+} is ~ 0.24 μM in aqueous solution in the absence of other salts and coordinating buffers,[23] while the corresponding value for Pb^{2+} is ~ 0.1 μM.[24] Clearly, the presence of Na^+, phosphate and acetate decreases the binding affinity of mTBA for the divalent metal ions compared to ideal conditions with no interfering species. However, our titration data is considered realistic, as metal ion sensors are met with a wide host of matrix effects,[1] including metal-coordinating salts and DNA-binding cations.

Our findings demonstrate the potential applications of fluorescent ICT-dG probes for aptasensor development in GQs. Of the two ICT probes tested, the turn-off vBthdG$_5$ nucleobase is the superior probe because it provides a much better response to toxic Pb^{2+} compared to K^+; ~ 8-fold difference in emission intensity (Fig. 2D), compared to a difference of only 1.9-fold for vAcPhdG (Fig. 2C). Despite vBthdG$_5$ exhibiting quenched emission upon Pb^{2+} binding, its emission sensitivity to Pb^{2+} suggests that ICT-DNA platforms may serve as effective sensors to detect Pb^{2+} in biological samples. In general, GQ-folding oligonucleotides exhibit good selectivity for Pb^{2+} because they display greater affinity for Pb^{2+} compared to K^+ or Na^+,[23,24,27] and other biological divalent metal ions such as Mg^{2+}, Ca^{2+}, Zn^{2+}, Cu^{2+} and Fe^{2+} bind GQ structures poorly.[12,14] Thus, further ICT probe development for incorporation into GQ-folding oligonucleotides is underway in an effort to improve emission sensitivity to Pb^{2+} and create an ICT-DNA platform that can meet the stringent detection limits (<50 nM) required for practical applications.[2,14]

Notes and references

1 D. W. Domaille, E. L. Que and C. J. Chang, *Nat. Chem. Biol.*, 2008, **4**, 168-175.
2 H. N. Kim, W. X. Ren, J. S. Kim and J. Yoon, *Chem. Soc. Rev.*, 2012, **41**, 3210-3244.
3 Z. Xu, Y. Xiao, X. Qian, J. Cui and D. Cui, *Org. Lett.*, 2005, **7**, 889-892.
4 X. Peng, J. Du, J. Fan, J. Wang, Y. Wu, J. Zhao, S. Sun and T. Xu, *J. Am. Chem. Soc.*, 2007, **129**, 1500-1501.
5 Y. Shiraishi, C. Ichimura, S. Sumiya and T. Hirai, *Chem. Eur. J.*, 2011, **17**, 8324-8332.
6 I. Willner, B. Shlyahovsky, M. Zayats and B. Willner, *Chem. Soc. Rev.*, 2008, **37**, 1153-1165.
7 P. Wu, K. Hwang, T. Lan and Y. Lu, *J. Am. Chem. Soc.*, 2013, **135**, 5254-5257.
8 R. Saran and J. Liu, *Anal. Chem.*, 2016, **88**, 4014-4020.
9 T. Li, S. Dong and E. Wang, *Anal. Chem.*, 2009, **81**, 2144-2149.
10 A. Dumas and N. W. Luedtke, *Chem. Eur. J.*, 2012, **18**, 245-254.
11 A. Omumi, C. K. McLaughlin, D. Ben-Israel and R. A. Manderville, *J. Phys. Chem. B*, 2012, **116**, 6158-6165.
12 T. Li, S. Dong and E. Wang, *J. Am. Chem. Soc.*, 2010, **132**, 13156–13157.
13 D. Li, S. P. Song and C. H. Fan, *Acc. Chem. Res.*, 2010, **43**, 631-641.
14 S. Zhan, Y. Wu, Y. Luo, L. Liu, L. He, H. Xing and P. Zhou, *Anal. Biochem.* 2014, **462**, 19-25.
15 A. C. Bhasikuttan and J. Mohanty, *Chem. Commun.*, 2015, **51**, 7581-7597.
16 S. Nagatoishi, T. Nojima, B. Juskowiak and S. Takenaka, *Angew. Chem. Int. Ed.*, 2005, **44**, 5067-5070.
17 S. Nagatoishi, T. Nojima, E. Galezowska, B. Juskowiak and S. Takenaka, *ChemBioChem*, 2006, **7**, 1730-1737.
18 R. F. Macaya, P. Schultze, F. W. Smith, J. A. Roe and J. Feigon, *Proc. Natl. Acad. Sci. USA*, 1993, **90**, 3745-3749.
19 D. J. M. Blanchard, K. L. Fadock, M. Sproviero, P. Deore, T. Z. Cservenyi, R. M. Manderville, P. Sharma and S. D. Wetmore, *J. Mat. Chem. C*, 2016. **4**, 2915-2924.
20 I. R. Krauss, A. Merlino, A. Randazzo, E. Novellino, L. Mazzarella and F. Sica, *Nucleic Acids Res.*, 2012, **40**, 8119-8128.
21 B. I. Kankia and L. A. Marky, *J. Am. Chem. Soc.*, 2001, **123**, 10799-10804.
22 X. Mao, L. A. Marky and W. H. Gmeiner, *J. Biomol. Struc. & Dyn.*, 2004, **22**, 25-33.
23 J. M. Wilcox, D. L. Rempel and M. L. Gross, *Anal. Chem.*, 2008, **80**, 2365-2371.
24 I. Smirnov and R. H. Shafer. *J. Mol. Biol.*, 2000, **296**, 1-5.
25 I. V. Smirnov, K. W. Kotch, I. J. Pickering, J. T. Davis and R. H. Shafer, *Biochemistry,* 2002, **41**, 12133-12139.
26 J. A. Mondragón-Sánchez, J. Liquier, R. H. Shafer and T. Taillandier, *J. Biomol. Struc. & Dyn.*, 2004, **22**, 365-373.
27 W. Liu, Y. Fu, B. Zheng S. Cheng, W. Li, T. Lau and H. Liang, *J. Phys. Chem. B*, 2011, **115**, 13051-13056.
28 D. J. M. Blanchard, T. Z. Cservenyi and R. A. Manderville, *Chem. Commun.*, 2015, **51**, 16829-16831.
29 UV thermal melting parameters, CD and emission spectra of GQ structures (6 μM) were recorded in 50 mM K^+-phosphate, pH 7.0 with 100 mM KCl, 10 mM PIPES, pH 7.0 with 5 mM $Ba(OAc)_2$ or $SrCl_2$ and 10 mM TRIS/acetate, pH 6.4 with 0.5 mM $Pb(NO_3)_2$.
30 Stock $SrCl_2$ and $Ba(OAc)_2$ solutions (30 mM) were prepared in 10 mM PIPES, pH 7.0 buffer, while stock $Pb(NO_3)_2$ was prepared in deionized water. Sr^{2+} and Ba^{2+} were added in 60 μM, while Pb^{2+} was added in 2 μM aliquots, in 5 min intervals until no further change in emission was detected.